ORIGINAL RESEARCH

Forensic Application of Postmortem Diffusion-Weighted and Diffusion Tensor MR Imaging of the Human Brain in Situ

E. Scheurer
K.-O. Lovblad
R. Kreis
S.E. Maier
C. Boesch
R. Dirnhofer
K. Yen

BACKGROUND AND PURPOSE: DWI and DTI of the brain have proved to be useful in many neurologic disorders and in traumatic brain injury. This prospective study aimed at the evaluation of the influence of the PMI and the cause of death on the ADC and FA for the application of DWI and DTI in forensic radiology.

MATERIALS AND METHODS: DWI and DTI of the brain were performed in situ in 20 deceased subjects with mapping of the ADC and FA. Evaluation was performed in different ROIs, and the influence of PMI and cause of death was assessed.

RESULTS: Postmortem ADC values of the brain were decreased by 49%–72% compared with healthy living controls. With increasing PMI, ADCs were significantly reduced when considering all ROIs together and, particularly, GM regions (all regions, $P < .05$; GM, $P < .01$), whereas there was no significant effect in WM. Concerning the cause of death, ADCs were significantly lower in mechanical and hypoxic brain injury than in brains from subjects having died from heart failure (traumatic brain injury, $P < .005$; hypoxia, $P < .001$). Postmortem FA was not significantly different from FA in living persons and showed no significant influence of PMI or cause of death.

CONCLUSIONS: Performing postmortem DWI and DTI of the brain in situ can provide valuable information for application in forensic medicine. ADC could be used as an indicator of PMI and could help in the assessment of the cause of death.

ABBREVIATIONS: ADC = apparent diffusion coefficient; ADC_{Tc} = temperature corrected apparent diffusion coefficient; CC = corpus callosum; DWI = diffusion-weighted imaging, DTI = diffusion tensor imaging; FA = fractional anisotropy; FSE = fast spin-echo; GM = gray matter, HF = cardiac failure; MRI = MR imaging; n.a. = measurements not performed; PMI = postmortem interval; ROI = region of interest; SEM = standard error of the mean; STIR = short tau inversion recovery; STR = strangulation; T_{app} =approximate body core temperature at the time of MR imaging; TBI = traumatic brain injury; WM = white matter

In DWI, signal intensity strongly depends on the rate of water diffusion, which can be used quantitatively to determine ADC.[1] The scalar FA derived from DTI adds detailed data on the average directionality of diffusion, which allows investigating connectivity and microstructural integrity of internal fibrous structures, such as neuronal tracts in the brain.[2-5] In clinical medicine, both DWI and DTI of the brain have proved to be useful particularly to assess ischemia, edema, and structural integrity in many neurologic disorders and in traumatic brain injury.[6-12]

In the past 10 years, radiologic methods such as CT and MR imaging have been increasingly used in forensic medicine to address, among others, neurotraumatologic and neuropathologic issues.[13-15] The application of DWI and DTI to the postmortem brain is expected to support the diagnosis of brain parenchyma damage due to traumatic incidents on a microstructural level by noninvasively revealing edema and rupture of fiber tracts.[16,17]

Numerous postmortem DWI and DTI studies were performed in the animal and human brain; however, most evaluated the effect of formalin fixation and PMI on diffusion properties[18-23] or investigated isolated fixed human brains for the diagnosis of disease.[24,25] To date, there are only very few studies on DWI or DTI in the postmortem unfixed human brain in situ that have concentrated on general characteristic changes in postmortem MR imaging and CT, including DWI on one hand and postmortem DTI in a single case with a brain stem trauma on the other.[17,26]

In this study, we aimed at the evaluation of a potential application of DWI and DTI and particularly ADC and FA in different regions of the postmortem brain in situ for the application in forensic diagnostics. The main goals were to assess the following: 1) whether there was an influence of the time since death on ADC and FA, which could be used for estimation of the PMI, and 2) whether there was a correlation with the cause of death.

Materials and Methods

Subjects

A consecutive sample of 20 deceased subjects with a forensic autopsy request by the legal authorities was included in this study (15 males, 5

Received October 22, 2010; accepted after revision December 17.

From the Ludwig Boltzmann Institute for Clinical-Forensic Imaging (E.S., K.Y.), Graz, Austria; Medical University Graz (E.S., K.Y.), Graz, Austria; Institute of Forensic Medicine (E.S., R.D., K.Y.), University of Bern, Bern, Switzerland; Department of Radiology (K.-O.L.), University of Geneva, Geneva, Switzerland; Department of Neuroradiology (K.-O.L.), Inselspital, Bern, Switzerland; Department of Clinical Research (R.K., C.B.), MR-Spectroscopy and -Methodology, University of Bern, Bern, Switzerland; and Department of Radiology (S.E.M.), Brigham and Women's Hospital, Harvard Medical School, Boston, Massachusetts.

Please address correspondence to Eva Scheurer, MD, MSc, Ludwig Boltzmann Institute for Clinical-Forensic Imaging, Universitätsplatz 4/II, A-8010 Graz, Austria; e-mail: eva.scheurer@cfi.lbg.ac.at

http://dx.doi.org/10.3174/ajnr.A2508

Indicates article with supplemental on-line table.

Table 1: Case data

Case	Age at Death [years]	Incident	Cause of Death[a]	Time of Death–MRI [hours]	T_{app}[b] [°C]
1	53	Fall from great height	Central respiratory arrest due to brain trauma	20	20
2	29	Natural death	Heart failure	44	20
3	94	Motor vehicle crash (pedestrian)	Central respiratory arrest due to brain trauma	45	10
4	63	Natural death	Heart failure	49	5
5	44	Diving accident	Heart failure due to gas embolism	51	5
6	45	Fall into a crevasse	Organ failure due to hypothermia	73	12
7	29	Suicidal hanging	Suffocation	13	30
8	79	Beating to death	Heart failure due to pneumothorax and fat embolism	14	28
9	30	Suicidal hanging	Suffocation	48	23
10	61	Motor vehicle crash (pedestrian)	Heart & lung failure due to blood aspiration and pneumothorax	49	10
11	19	Incidental gas intoxication (propane & butane)	Central respiratory arrest	14	25
12	46	Manual strangulation	Suffocation	14	22
13	3	Natural death	Central respiratory arrest due to suffocation (laryngitis)	19	8
14	46	Suicidal intoxication & hypothermia	Central respiratory arrest and hypothermia (combined)	33	5
15	37	Natural death	Heart failure	17	8
16	28	Incidental hanging	Suffocation	141	5
17	58	Natural death	Heart failure	25	10
18	29	Suicidal hanging	Suffocation	61	15
19	58	Medical maltreatment	Heart failure due to arterial air embolism	43	10
20	49	Hang-glider crash	Central respiratory insufficience due to brain stem lesion	27	19

[a] In cases with combined or concurring causes of death only the most relevant are mentioned.
[b] Approximate body core temperature at the time of MR imaging

females; mean age, 45 years; median, 46 years; age range, 3–94 years). Two healthy living volunteers (a man, aged 26 years; a woman, aged 31 years) were examined as controls. Before scanning, the corpses were examined externally by a forensic pathologist to ensure compliance with the inclusion criteria (ie, PMI at the time of inclusion <120 hours, no signs of decomposition, no history of neurologic disorder). PMI was determined either by witnessed death (eg, when death occurred in hospital) or by standard forensic methods (body temperature, livor and rigor mortis). For the evaluation of the quantitative effect of PMI, subjects were divided into 3 groups: PMI group 1, with PMI ≤24 hours ($n = 7$; mean age ± SEM, 38 ± 22.8 years), PMI group 2 with PMI 25–48 hours ($n = 7$, age, 52 ± 20.3 years), PMI group 3 with PMI >48 hours ($n = 6$, age, 45 ± 13.7 years). Mean ages in the groups were not significantly different from each other. In 12 subjects, the cause of death, as diagnosed at forensic autopsy after scanning, was traumatic; 3 had died from intoxication or medical maltreatment, and 5 from natural causes (Table 1). For the analysis of the influence of the cause of death, subject groups were defined as the following: 1) mechanical brain trauma ($n = 4$), with all subjects showing signs of a direct blunt force impact and intracranial hemorrhage and varying additional findings, such as skull fractures, cerebral contusions, and edema; 2) hypoxic brain injury caused by strangulation ($n = 5$); and 3) heart failure ($n = 4$). The study was approved by the local ethics committee, and informed consent was obtained from the living volunteers.

MR Imaging

MR imaging of the brain in situ was performed within 141 hours after death (mean, 40 hours; median, 38 hours; range, 13–141 hours) at 1.5T (Signa EchoSpeed Horizon, Version 5.8; GE Healthcare, Milwaukee, Wisconsin) by using a quadrature head coil. Depending on cooling time at 4°C, body core temperature at the beginning of the acquisition was between 5°C and 30°C (median, 11°C). The measurement was performed with a digital thermometer in the rectum. For MR imaging, the bodies were wrapped in 2 artifact-free body bags to prevent contamination and to guarantee anonymity.

Data were acquired in the axial orientation with a multisection line-scan sequence; for each section, 6 images with high b-values ($b_{max} = 1000$ s/mm^2) in 6 noncollinear and noncoplanar directions [relative amplitudes: $(G_x,G_y,G_z) = \{(1,1,0),(0,1,1),(1,0,1)(-1,1,0),(0,-1,1)(1,0,-1)\}$] and 2 images with low b-values (5 s/mm^2) were obtained. The imaging parameters were the following: TR/TE, 3520/96 ms; matrix, 128 × 128; FOV, 24 × 24 cm; NEX, 1; sections, 22; section thickness, 5 mm; section gap, 1 mm. Additionally, a standard protocol, including an axial T1-weighted (TR/TE, 400/14 ms), T2-weighted FSE (TR/TE, 4000/15 ms), STIR (TR/TE, 11 002/217 ms), and a fast multiplanar spoiled gradient-recalled acquisition in the steady state (TR/TE, 270/4.2 ms) sequence, was performed. Total scanning times ranged from 35 to 75 minutes.

For the living volunteers, the same protocol with parameters typical for in vivo examinations was used (DTI: TR/TE, 3392/84.5 ms; matrix, 128 × 128; FOV, 22 × 22 cm; NEX, 1; sections, 12; section thickness, 5 mm; section gap, 6 mm; and b_{max}, 1000 s/mm^2).

Data analysis was performed on an Advantage Windows workstation (Version 9.1, GE Healthcare).

Evaluation of ADC and FA

Maps of ADC and FA were calculated on a pixel-by-pixel basis after zero-filling to a matrix size of 256 × 256. Quantitative measurements were performed by 2 independent examiners (neuroradiologist, 11 years of experience; forensic expert, 10 years of experience) section by section in anatomically specified ROIs (circular ROIs for ADC, 10 mm^2; for FA, 20 mm^2, respectively). ADC was measured bilaterally in 20 ROIs in GM and WM as well as regions with mixed proportions (ie, fractions of both white and gray matter, as listed in the On-line Table) and 1 ROI in the cerebellar vermis (Fig 1); FA was measured bilaterally in 9 ROIs in WM and mixed regions only (Table 2). For statistical evaluation, the ROIs were grouped in WM, GM, and all ROIs (ie, including ROIs with mixed tissue). Because diffusion is temperature-dependent, ADCs of the postmortem cases were temperature-corrected to 38°C by using a correction factor of 2% per degree Celsius according to the equation[27]: $ADC_{Tc} = ADC(100\% +$

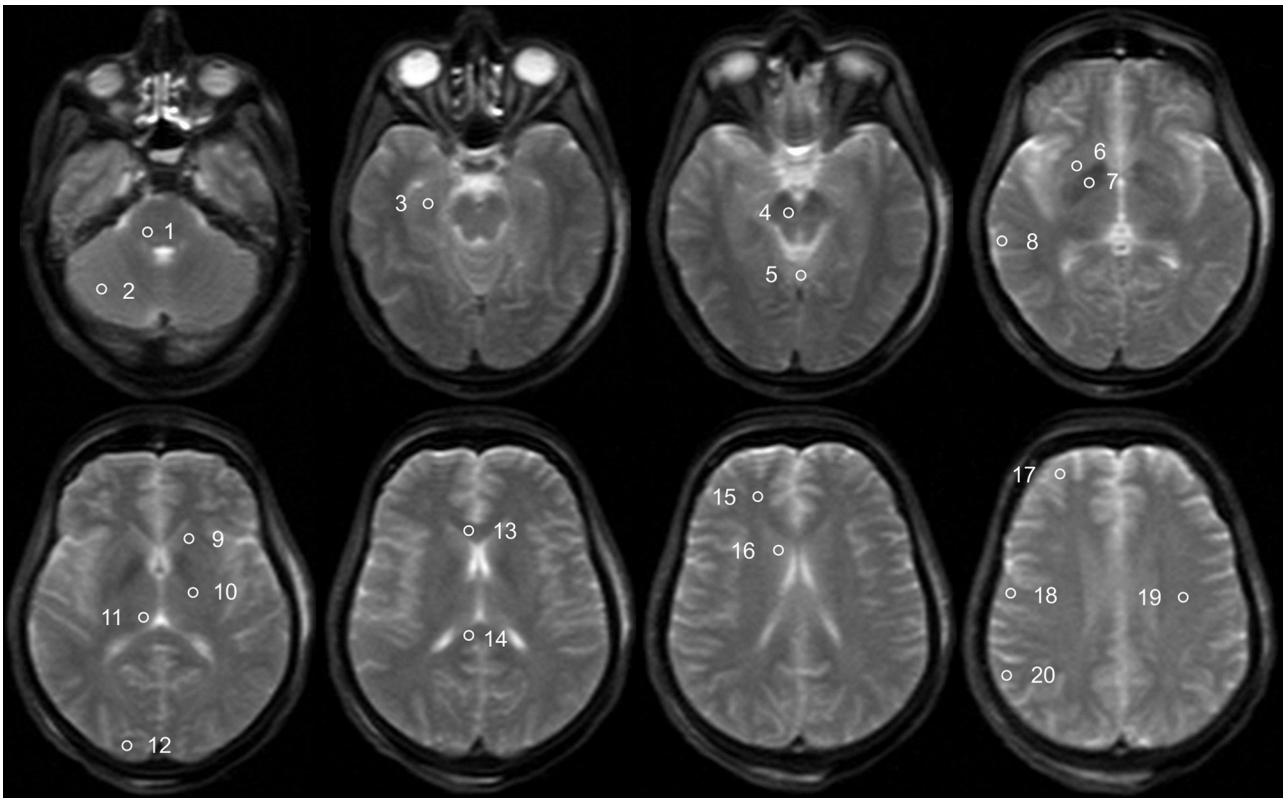

Fig 1. Trace-weighted image (b-value = 5 s/mm^2) of a deceased subject showing the placement of ROIs for the evaluation of ADC values. ROIs are only shown unilaterally; the ROI in the medulla is not shown. The ROIs are the following: 1) pons, 2) cerebellum, 3) hippocampus, 4) mesencephalon, 5) vermis, 6) putamen, 7) pallidum, 8) temporal cortex, 9) internal capsule anterior, 10) internal capsule posterior, 11) thalamus, 12) occipital cortex, 13) corpus callosum genu, 14) corpus callosum splenium, 15) frontal WM, 16) caudate nucleus, 17) frontal cortex, 18) motor cortex, 19) centrum semiovale, and 20) parietal cortex.

Table 2: FA in different ROIs

	FA						
	Postmortem Cases[a]					Living Controls	
ROI	Mean	SD	Median	Min	Max	Mean	SD
Frontal white matter	0.25	0.05	0.25	0.15	0.34	0.22	0.01
Centrum semiovale	0.26	0.04	0.25	0.18	0.34	0.32	0.03
Internal capsule anterior	0.31	0.07	0.31	0.18	0.41	0.32	0.02
Internal capsule posterior	0.41	0.04	0.41	0.33	0.51	0.36	0.01
Corpus callosum genu	0.36	0.08	0.37	0.19	0.48	0.36	0.04
Corpus callosum splenium	0.49	0.08	0.51	0.32	0.59	0.56	0.04
Mesencephalon	0.31	0.05	0.30	0.24	0.49	0.43	0.03
Pons	0.31	0.05	0.31	0.23	0.39	0.31	0.04
Medulla	0.22	0.04	0.22	0.16	0.28	n.a.	n.a.

[a] Given are the mean, standard deviation, median, minimum, and maximum except case 9 (n = 19).

2%)$^{(38°C\text{-}Tapp)}$. The body core temperature measured at the start of the scan (T_{app}) was used for the correction.

Forensic Autopsy and Histology

After MR imaging, autopsy was performed by 2 forensic pathologists within 24 hours, in 2 cases a few hours later (34 and 44 hours, respectively). Autopsy included detailed neuropathologic evaluation in all cases; histologic examination was performed from visible lesions. Visual comparison of MR images with autopsy findings and, if available, with their histologic correlates was performed.

Statistical Analysis

For analysis, ADC and FA measurements of both examiners were pooled for each ROI. The evaluation of effects of PMI and cause of death was performed with the Statistical Package for the Social Sciences, Version 17.0 (SPSS, Chicago, Illinois) by using a univariate analysis of variance with a Bonferroni post hoc correction for multiple tests (pair-wise comparisons). A P value of $< .05$ was considered significant. The brain regions were assigned to 3 groups (GM, WM, mixed) as shown in the On-line Table. The effect of PMI on ADC was evaluated once for all brain regions with PMI group and brain region as factors. A second analysis was calculated separately for GM and WM regions, respectively, with the PMI group as a factor. Additionally, the Pearson correlation of PMI and ADC was evaluated (2-sided). For the assessment of the effect of PMI on FA, only the PMI group was used as a factor because only WM and mixed tissue ROIs had been measured. The influence of a cause of death involving mechanical or hypoxic brain injury on ADC was assessed with cause of

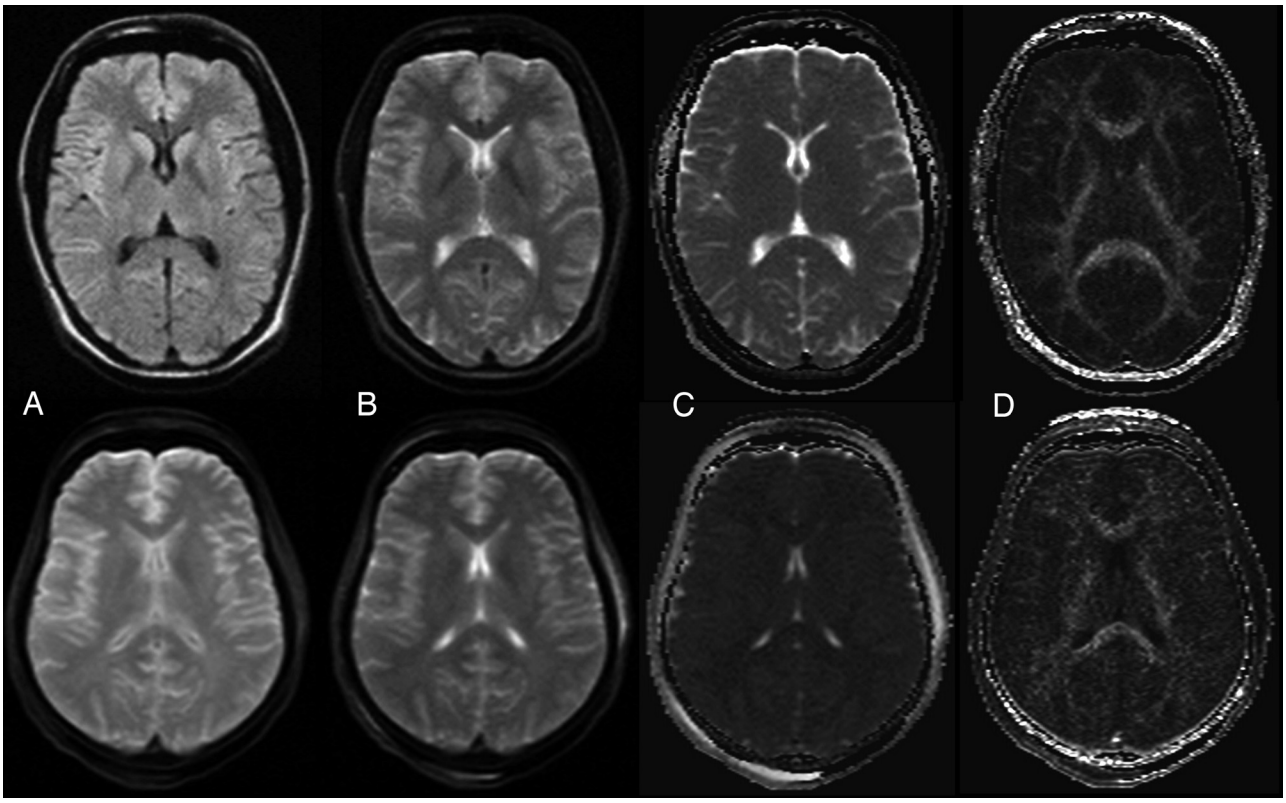

Fig 2. Example of a DWI image, b_0 image, ADC map, and FA map of a healthy living volunteer (woman, 31 years) (top row) and a deceased subject (woman; age, 45 years; PMI, 73 hours; body temperature at acquisition, 12°C) (bottom row). *A*, DWI (b = 1000 s/mm^2). *B*, Trace-weighted image with b-value = 5 s/mm^2. *C*, ADC map. *D*) FA map.

death and brain region as factors, while for the effect on FA, only cause of death was used as a factor.

Results

ADC

Good-quality DWI and DTI were acquired in deceased subjects as well as in healthy living volunteers. Figure 2 shows an example of postmortem and in vivo DWI and the ADC and FA maps in the respective subjects.

The On-line Table summarizes mean, SD, median, and minimal and maximal values for the ADC_{Tc} in different brain regions in comparison with ADCs of the living controls. Mean postmortem ADC_{Tc} ranged from 21 $\times$ 10^{-5}mm^2/s (vermis of the cerebellum) to 41 $\times$ 10^{-5}mm^2/s (medulla). Postmortem ADC_{Tc} of GM with a mean ADC_{Tc} between 34 $\times$ 10^{-5}mm^2/s (frontal cortex) and 38 $\times$ 10^{-5}mm^2/s (occipital cortex) was significantly higher than ADC_{Tc} values in WM ($P < .01$) with a mean ADC_{Tc} between 29 $\times$ 10^{-5}mm^2/s (centrum semiovale) and 41 $\times$ 10^{-5}mm^2/s (medulla) and in mixed regions ($P < .05$). Compared with the ADCs of the living volunteers, which ranged from 67 $\times$ 10^{-5}mm^2/s (cerebellum) to 81 $\times$ 10^{-5}mm^2/s (hippocampus), postmortem ADC_{Tc} was considerably reduced. The greatest decrease was observed in the vermis, with a reduction of 72% compared with the ADC of the healthy living controls, while the least reduction was 49% in the occipital cortex.

Figure 3 compares the ADCs of the living controls with the postmortem values and shows the great decrease in all examined ROIs. In contrast to this huge effect, approximate temperature correction had only a minor influence.

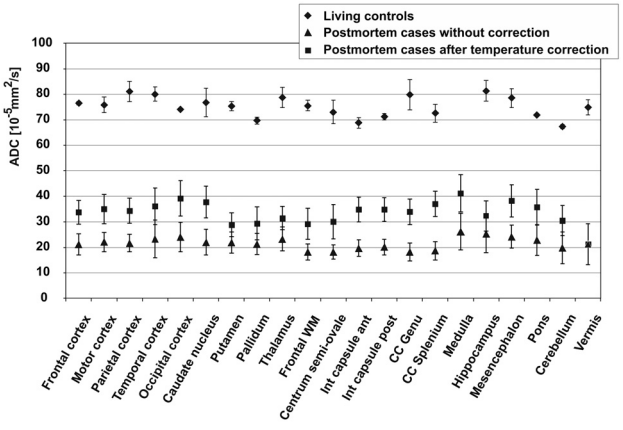

Fig 3. Comparison of ADC of the postmortem cases with the living controls and demonstration of the effect of temperature correction on postmortem ADC. Data points are mean values for the respective ROI; error bars show the corresponding SD.

To evaluate the effect of the PMI on the ADC_{Tc} of different brain regions, we compared 3 groups. Group 1 had a mean PMI of 16 hours (SD, 3 hours; median, 14 hours; range, 13–20 hours), group 2 a mean PMI of 38 hours (SD, 9 hours; median, 43 hours; range, 25–48), and group 3 a mean PMI of 71 hours since death (SD, 36 hours; median, 56 hours; range, 49–141 hours). Within the 3 groups, the distribution of the causes of death (brain trauma, strangulation, and heart failure) was not significantly different. Figure 4 shows that with increasing PMI, postmortem ADC_{Tc} in the overall brain and in GM regions decreased significantly between group 1 and group 3 (all ROIs, $P < .05$; GM, $P < .01$), while there were no significant

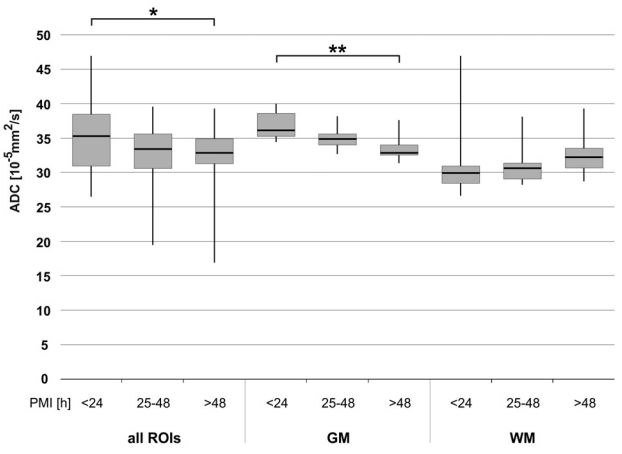

Fig 4. Influence of PMI on ADC_{Tc} in all ROIs, GM, and WM, respectively. Whiskers show the maximum and the minimum values. A single asterisk indicates $P < .05$; double asterisks, $P < .01$.

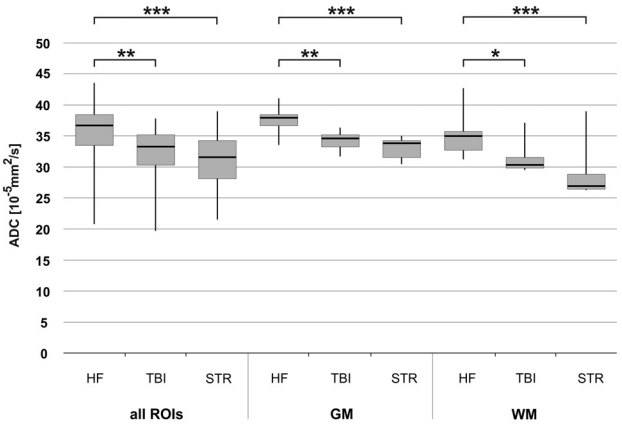

Fig 5. Influence of mechanical brain trauma and hypoxic brain injury due to strangulation on ADC_{Tc} of all ROIs, GM, and WM, respectively. A group of brain trauma cases ($n = 4$) and a group of strangulation cases ($n = 5$) are compared with a group of subjects with natural death due to cardiac failure ($n = 4$). Whiskers show the maximum and the minimum values. A single asterisk indicates $P < .05$; double asterisks, $P < .005$; and triple asterisks, $P < .001$.

differences between groups 1 and 2, or between groups 2 and 3. In WM regions, no significant effect was observable. Correlation of ADC with PMI showed a decreasing linear trend; however, with a moderate and not statistically significant correlation coefficient of $r = 0.42$ for GM ($P = .06$).

The influence of the cause of death on the ADC_{Tc} in all ROIs and in GM and WM separately is demonstrated in Fig 5. The subjects having died from a natural cause due to cardiac failure had significantly higher ADC_{Tc} values in all brain regions than those who died from mechanical brain trauma (all ROIs, $P < .005$; GM, $P < .005$; WM, $P < .05$) or the subjects with hypoxic brain injury due to congestion resulting from strangulation (all ROIs, $P < .001$; GM, $P < .001$; WM, $P < .001$). There was no significant difference between the 2 types of brain injury, and no correlation between the cause of death and PMI.

FA

Between the deceased subjects and the living controls, there was no significant difference concerning FA of all brain regions (Fig 6). Mean values were between 0.22 and 0.49 in the

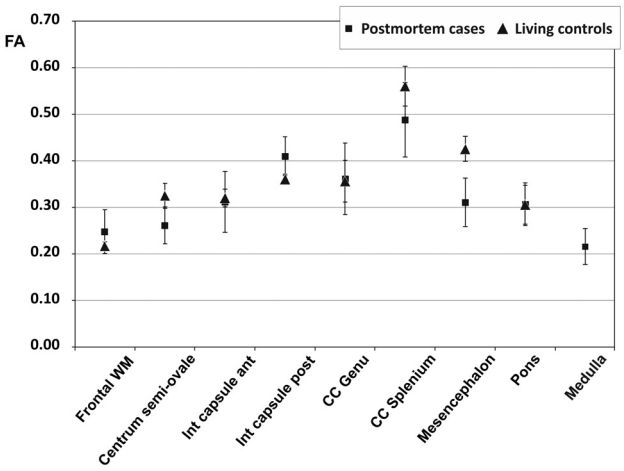

Fig 6. Comparison of FA of the postmortem cases with the living controls in different brain regions. Data points are mean values for the respective ROI; error bars show the corresponding SD.

postmortem cases and between 0.22 and 0.56 in the living controls (Table 2). The highest FA was measured in the splenium of the corpus callosum in both postmortem and living subjects, while the lowest value was found in the medulla and frontal WM. The PMI did not have any significant effect on FA (ie, the pair-wise comparisons among the 3 groups of subjects did not show any significant difference [Fig 7*A*]). FA was also stable regarding the influence of different types of brain injury (ie, mechanical brain trauma and hypoxic injury due to strangulation). None of the pair-wise comparisons reached significance when comparing the subjects with brain injury with those having died from cardiac failure (Fig 7*B*).

Traumatologic Changes

In 6 cases, traumatic changes of the brain were observed at autopsy, which were mainly intracerebral hematoma ($n = 1$), lacerations ($n = 3$), and subarachnoid ($n = 8$) and subdural hematomas ($n = 3$). Of these, 4 subarachnoid hemorrhages and 1 thin subdural blood layer were not seen on MR imaging. All other findings were detected with MR imaging with a good correlation to autopsy.

Discussion

ADC and FA were measured in the postmortem brain in situ to evaluate DWI and DTI for forensic application. Visual comparison of postmortem ADC maps with those in the living controls already showed clearly reduced diffusivity. Although differences in body temperature could well be one reason for this, postmortem ADC_{Tc} proved to be significantly decreased compared with the values of living subjects in all brain regions, confirming previous studies,[26,28] agreeing also with clinical findings in acute ischemia due to cerebral occlusion.[29-31] Postmortem ADC_{Tc} values were significantly higher in GM than in WM. Because this observation was also reported in living subjects,[32] this difference between gray and white matter seems to be preserved postmortem.

In forensic medicine, PMI (ie, the time span between death and either examination or fixation) is essential for criminal investigations. Particularly beyond approximately 30 hours after death, when the body reaches ambient temperature,

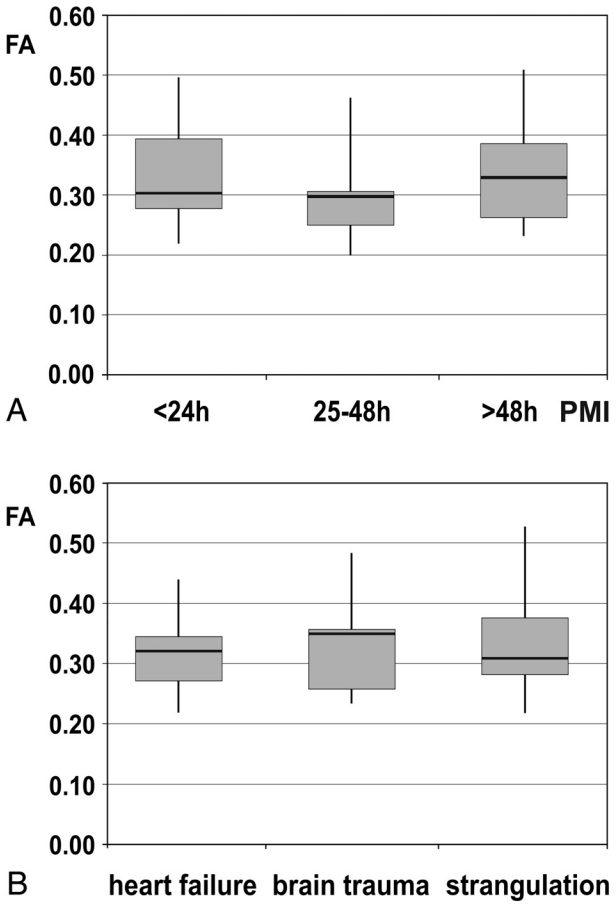

Fig 7. *A*, Influence of the PMI on FA in 3 groups of subjects (PMI < 24 hours, $n = 7$; PMI = 25–48 hours, $n = 7$; PMI > 48 hours, $n = 6$). Whiskers show the maximum and the minimum values. *B*, Effect of the cause of death—that is, mechanical brain trauma and hypoxic injury of the brain due to strangulation compared with heart failure—on FA. Whiskers show the maximum and the minimum values.

objective methods are hardly developed.[33,34] A significant difference of ADC_{Tc} was found mainly in the GM between the group with PMIs ≤1 day and that with PMIs of >2 days. This is in agreement with previous studies that investigated the effect of PMI in tissue samples of animal brain fixed at different time points after death.[20,22] However, in contrast to these studies, no significant effect of PMI on ADC could be observed for WM. Linear correlation of ADC with PMI was moderate, which can be attributed to several reasons such as an overlay by the differences in the cause of death, incomplete data with higher PMIs, as well as an influence of noise and imperfect temperature correction. Additionally, the decrease may be nonlinear. However, the measurement of postmortem ADC_{Tc} in GM could emerge as a valuable method for a noninvasive and objective estimation of PMI.

Regarding the cause of death, ADC_{Tc} was significantly lower in all brain regions in 2 groups of subjects, with a cause of death associated with brain injury compared with subjects with cardiac failure. No significant difference between brain injury caused by mechanical trauma and hypoxic injury due to strangulation was found. The higher ADC_{Tc} in subjects with heart failure could be an indicator of the length of the process of dying (ie, agony). This would be in good agreement with the ADC_{Tc} values in the groups with brain injury, because according to forensic experience, agony is usually prolonged to several minutes in death due to cardiac failure, while in strangulation agony is expected to be very short, in some cases even shorter than in death due to mechanical brain trauma. In forensic medicine, the assessment of the cause of death can be challenging, particularly in cases without any exteriorly visible injuries. Thus, postmortem ADC_{Tc} could help in noninvasively differentiating natural death from death caused by occult brain injury mechanisms. Because ADC in WM seems to be less influenced by PMI, the evaluation of WM regions would be preferential to address this question.

Postmortem FA did not change significantly compared with the values of the healthy living volunteers. Additionally, PMI and the presence of brain injury did not show any significant change of FA. This observation disagrees with those in other studies, which found decreasing anisotropy following brain death.[22,23,35-37] However, direct comparison is difficult because in some of these studies, fixed brain or tissue samples were used while we examined entire unfixed brains in situ. An effect of fixation on most diffusivity indices has been shown but obviously does not affect all indices and locations of the brain equally.[18,20,21,23] Small effects of PMI on FA may have been hidden by using all ROIs containing WM and mixed tissue; however, the obviously inconsistent effect of death on FA as seen in Fig 4 does not support such speculation. The FA values found in the healthy living volunteers were lower than those reported previously.[11,38] This was probably caused by averaging over large ROIs with contamination by GM and WM regions with fiber crossings.

While most traumatic findings were seen in MR imaging, the detection of thin blood layers seems to be difficult. This is in agreement with previous results.[39]

Regarding limitations of this study, the influence of age, sex, and hemispheric differences was not evaluated because there were no significant differences between the investigated groups and, additionally, because they seem to have no or limited impact.[28,32,40] The sample size of the investigated subjects was limited, and there is a need for corroboration of the results, particularly for the evaluation of the cause of death and a possible influence of agony. To minimize the effect of varying brain temperatures as a consequence of PMI, approximate temperature correction was performed. However, only body core temperature was available, which might differ from brain temperature. The cortical ADC measurements may have been influenced by partial volume effects with the surrounding CSF. Additionally, given the strongly reduced postmortem ADCs found in this study, the definition of ADC and FA would be more accurate if a much higher maximum b-value could be chosen than is normally used in vivo. For example, with the current finding of ADC_{Tc} being about half the in vivo value, a 3.5 times higher maximum b-value should be used at 10°C to reach a diffusion weighting comparable with in vivo. Whether this is possible with the same TE depends on the technically achievable gradient strengths of a particular MR imaging scanner.

Conclusions

Postmortem DWI of the brain in situ has the potential to improve forensic diagnostics, specifically regarding PMI estimation and definition of the cause of death. Additionally, the fact

that the brain seems to remain structurally intact in the early postmortem period is relevant for future postmortem imaging studies.

References

1. Le Bihan D, Breton E, Lallemand D, et al. **MR imaging of intravoxel incoherent motions: application to diffusion and perfusion in neurologic disorders.** *Radiology* 1986;161:401–07
2. Basser PJ, Pierpaoli C. **Microstructural and physiological features of tissues elucidated by quantitative-diffusion-tensor MRI.** *J Magn Reson B* 1996;111:209–19
3. Moseley ME, Cohen Y, Kucharczyk J, et al. **Diffusion-weighted MR imaging of anisotropic water diffusion in cat central nervous system.** *Radiology* 1990;176:439–45
4. Pierpaoli C, Jezzard P, Basser PJ, et al. **Diffusion tensor MR imaging of the human brain.** *Radiology* 1996;201:637–48
5. Le Bihan D, Mangin JF, Poupon C, et al. **Diffusion tensor imaging: concepts and applications.** *J Magn Reson Imaging* 2001;13:534–46
6. Warach S, Gaa J, Siewert B, et al. **Acute human stroke studied by whole brain echo planar diffusion-weighted magnetic resonance imaging.** *Ann Neurol* 1995;37:231–41
7. Sorensen AG, Wu O, Copen WA, et al. **Human acute cerebral ischemia: detection of changes in water diffusion anisotropy by using MR imaging.** *Radiology* 1999;212:785–92
8. Moonen CT, Pekar J, de Vleeschouwer MH, et al. **Restricted and anisotropic displacement of water in healthy cat brain and in stroke studied by NMR diffusion imaging.** *Magn Reson Med* 1991;19:327–32
9. Horsfield MA, Jones DK. **Applications of diffusion-weighted and diffusion tensor MRI to white matter diseases: a review.** *NMR Biomed* 2002;15:570–77
10. Filippi CG, Lin DD, Tsiouris AJ, et al. **Diffusion-tensor MR imaging in children with developmental delay: preliminary findings.** *Radiology* 2003;229:44–50
11. Huisman TA, Schwamm LH, Schaefer PW, et al. **Diffusion tensor imaging as potential biomarker of white matter injury in diffuse axonal injury.** *AJNR Am J Neuroradiol* 2004;25:370–76
12. Schaefer PW, Huisman TA, Sorensen AG, et al. **Diffusion-weighted MR imaging in closed head injury: high correlation with initial Glasgow coma scale score and score on modified Rankin scale at discharge.** *Radiology* 2004;233:58–66
13. Thali MJ, Yen K, Schweitzer W, et al. **Virtopsy, a new imaging horizon in forensic pathology: virtual autopsy by postmortem multislice computed tomography (MSCT) and magnetic resonance imaging (MRI)—a feasibility study.** *J Forensic Sci* 2003;48:386–403
14. Yen K, Sonnenschein M, Thali MJ, et al. **Postmortem multislice computed tomography and magnetic resonance imaging of odontoid fractures, atlantoaxial distractions and ascending medullary edema.** *Int J Legal Med* 2005;119:129–36
15. Aghayev E, Yen K, Sonnenschein M, et al. **Virtopsy post-mortem multi-slice computed tomography (MSCT) and magnetic resonance imaging (MRI) demonstrating descending tonsillar herniation: comparison to clinical studies.** *Neuroradiology* 2004;46:559–64
16. Jones NR, Blumbergs PC, Brown CJ, et al. **Correlation of postmortem MRI and CT appearances with neuropathology in brain trauma: a comparison of two methods.** *J Clin Neurosci* 1998;5:73–79
17. Yen K, Weis J, Kreis R, et al. **Line-scan diffusion tensor imaging of the posttraumatic brain stem: changes with neuropathologic correlation.** *AJNR Am J Neuroradiol* 2006;27:70–73
18. Sun SW, Neil JJ, Song SK. **Relative indices of water diffusion anisotropy are equivalent in live and formalin-fixed mouse brains.** *Magn Reson Med* 2003;50:743–48
19. Sun SW, Neil JJ, Liang HF, et al. **Formalin fixation alters water diffusion coefficient magnitude but not anisotropy in infarcted brain.** *Magn Reson Med* 2005;53:1447–51
20. D'Arceuil H, de Crespigny A. **The effects of brain tissue decomposition on diffusion tensor imaging and tractography.** *Neuroimage* 2007;36:64–68
21. Sun SW, Liang HF, Xie M, et al. **Fixation, not death, reduces sensitivity of DTI in detecting optic nerve damage.** *Neuroimage* 2009;44:611–19
22. Shepherd TM, Flint JJ, Thelwall PE, et al. **Postmortem interval alters the water relaxation and diffusion properties of rat nervous tissue: implications for MRI studies of human autopsy samples.** *Neuroimage* 2009;44:820–26
23. Schmierer K, Wheeler-Kingshott CA, Tozer DJ, et al. **Quantitative magnetic resonance of postmortem multiple sclerosis brain before and after fixation.** *Magn Reson Med* 2008;59:268–77
24. Larsson EM, Englund E, Sjobeck M, et al. **MRI with diffusion tensor imaging post-mortem at 3.0 T in a patient with frontotemporal dementia.** *Dement Geriatr Cogn Disord* 2004;17:316–19
25. Englund E, Sjobeck M, Brockstedt S, et al. **Diffusion tensor MRI post mortem demonstrated cerebral white matter pathology.** *J Neurol* 2004;251:350–52
26. Kobayashi T, Shiotani S, Kaga K, et al. **Characteristic signal intensity changes on postmortem magnetic resonance imaging of the brain.** *Jpn J Radiol* 2010;28:8–14
27. Quesson B, de Zwart JA, Moonen CT. **Magnetic resonance temperature imaging for guidance of thermotherapy.** *J Magn Reson Imaging* 2000;12:525–33
28. Naganawa S, Sato K, Katagiri T, et al. **Regional ADC values of the normal brain: differences due to age, gender, and laterality.** *Eur Radiol* 2003;13:6–11
29. Schlaug G, Siewert B, Benfield A, et al. **Time course of the apparent diffusion coefficient (ADC) abnormality in human stroke.** *Neurology* 1997;49:113–19
30. Lovblad KO, Bassetti C. **Diffusion-weighted magnetic resonance imaging in brain death.** *Stroke* 2000;31:539–42
31. Weber J, Mattle HP, Heid O, et al. **Diffusion-weighted imaging in ischaemic stroke: a follow-up study.** *Neuroradiology* 2000;42:184–91
32. Helenius J, Soinne L, Perkio J, et al. **Diffusion-weighted MR imaging in normal human brains in various age groups.** *AJNR Am J Neuroradiol* 2002;23:194–99
33. Ith M, Bigler P, Scheurer E, et al. **Observation and identification of metabolites emerging during postmortem decomposition of brain tissue by means of in situ 1H-magnetic resonance spectroscopy.** *Magn Reson Med* 2002;48:915–20
34. Scheurer E, Ith M, Dietrich D, et al. **Statistical evaluation of time-dependent metabolite concentrations: estimation of post-mortem intervals based on in situ 1H-MRS of the brain.** *NMR Biomed* 2005;18:163–72
35. Pfefferbaum A, Sullivan EV, Adalsteinsson E, et al. **Postmortem MR imaging of formalin-fixed human brain.** *Neuroimage* 2004;21:1585–95
36. Schmierer K, Wheeler-Kingshott CA, Boulby PA, et al. **Diffusion tensor imaging of post mortem multiple sclerosis brain.** *Neuroimage* 2007;35:467–77
37. Watanabe T, Honda Y, Fujii Y, et al. **Serial evaluation of axonal function in patients with brain death by using anisotropic diffusion-weighted magnetic resonance imaging.** *J Neurosurg* 2004;100:56–60
38. Tollard E, Galanaud D, Perlbarg V, et al. **Experience of diffusion tensor imaging and 1H spectroscopy for outcome prediction in severe traumatic brain injury: preliminary results.** *Crit Care Med* 2009;37:1448–55
39. Anon J, Remonda L, Spreng A, et al. **Traumatic extra-axial hemorrhage: correlation of postmortem MSCT, MRI, and forensic-pathological findings.** *J Magn Reson Imaging* 2008;28:823–36
40. Engelter ST, Provenzale JM, Petrella JR, et al. **The effect of aging on the apparent diffusion coefficient of normal-appearing white matter.** *AJR Am J Roentgenol* 2000;175:425–30